CHINA FOUNDRY Research & Development
Vol. 17 No. 5 September 2020
https://doi.org/10.1007/s41230-020-0012-8

Influence of Al-B grain refiner on porosity formation of directionally solidified Al-Si alloys

***Muhammet Uludağ**

Bursa Technical University, Metallurgical and Materials Engineering Department, Bursa, Turkey

Abstract: This work aims to present a perspective for porosity formation in three different alloys: A356, A413 and A380.1 by taking into account the addition of Al-B grain refiners: $AlTi_5B_1$ and Al_3B. The directional solidification method was used, and microstructural changes of the alloys and its correlation with porosity formation were investigated. Pore size, number of pores, average pore length and distribution of pores were statistically analyzed. Also, external shrinkage was examined, and the volume of external shrinkage was calculated. It was found that there was a relationship between external shrinkage and the size and number of pores. As the size and number of pores internally decrease, external shrinkage increases. Additionally, porosity is decreased in all the three Al-Si alloys when Al-B grain refiners are used. The distribution of pore diameters is low when $AlTi_5B_1$ is used. Grain refiners have a different effect on porosity formation of Al-Si alloys with regard to their solidification morphology.

Key words: Al-Si alloys; directional solidification; grain refinement; internal porosity; external shrinkage

CLC numbers: TG146.21 **Document code:** A **Article ID:** 1672-6421(2020)05-372-06

Aluminum alloys are preferred by the automotive industry due to their properties such as good castability, high strength and corrosion resistance [1]. These properties are mainly influenced by microstructure [2, 3]. Changes in microstructure can also affect porosity formation [4-7]. It is well known that the addition of Al-Ti-B master alloy into an Al-Si alloy will alter the microstructure from coarse α-Al to finer equiaxed dendritic morphology without changing the eutectic silicon morphology [8]. When it comes to the selection of master alloy, Al_3Ti_3B and Al_5Ti_1B grain refiners were compared in terms of effect on both microstructure and porosity formation [9]. It was concluded that Al_3Ti_3B grain refiner has a greater effect to prevent the porosity than Al_5Ti_1B grain refiner. As an alternative Al-Ti grain refiner of Al alloys, Al_3B master alloy that contains no Ti was also studied. This master alloy contains B, AlB_2 and AlB_{12} particles. AlB_{12} can be unstable depending on the B content of the melt and reacts with Al to form AlB_2 which is a peritectic reaction [10, 11]. In casting applications, it has been reported that AlB_2 addition results in more globular dendrites than the addition of TiB_2 [12]. Furthermore, AlB_2 has a great effect on porosity formation [12]. A previous study by Uludağ et al. [13] shows that titanium-free grain refiner addition yields lower porosity in Al alloys while titanium addition reveals higher volumetric porosity formation. Therefore, the characterization of grain refiners and their effect on porosity formation has been a great debate among researchers. Dong et al. [9, 14] claimed that grain refiners had a crucial effect on porosity formation, and the porosity was found to be decreased in Al_3Ti_3B grain refined hypoeutectic Al-Si alloy. It was shown that minimum porosity was obtained in Al-15Zn-2.5Mg-2.5Cu alloy when 1% $AlTi_5B_1$ was used [15]. Yüksel et al.[16, 17] claimed that as long as the grains are smaller, a porosity-free structure can be achieved. Roy et al. [18] claimed that pores were observed around TiB_2 particles. In another study by Spittle [19], it was mentioned that porosity can be decreased without the need for grain refinement. On the other hand, there are limited number of works concerning the correlation between B-grain refined cast Al alloys and their effect on porosity formation. Dispinar et al. [12] had reported that pores had become more localized in Ti-free B grain refined A356 alloy. Therefore, in this work, three different alloys (A356, A413, A380.1) that have different solidification morphologies were grain refined with $AlTi_5B_1$ and Al_3B, respectively. The relationship between the grain refinement and porosity formation for the three different alloys was investigated to fill the blank in the literature.

***Muhammet Uludağ**

Male, born in 1982, Ph.D, Assistant Professor, Researcher. His research interests mainly focus on aluminum alloys, high pressure die casting process, improvement of casting quality and mechanical properties, microstructural characterization, heat treatment of aluminum alloys, and casting simulation. To date, he has published 25 technical papers in journals and more than 80 proceedings papers.

E-mail: dr.uludagm@gmail.com

Received: 2020-02-01; Accepted: 2020-06-23

1 Experimental procedure

Chemical compositions of A356, A413 and A380.1 alloys used in this study are given in Table 1. A water-cooled copper chilled cylindrical mould was used in the experiments. The directional solidification apparatus is shown in Fig. 1, and the dimension of the die was 30 mm in diameter and 300 mm in length.

Table 1: Chemical compositions of experimental alloys (wt.%)

Alloys	Si	Fe	Cu	Mn	Mg	Zn	Ti	Al
A356	6.80	0.19	0.003	0.001	0.30	0.011	0.108	Bal.
A413	11.77	0.19	0.006	0.001	0.005	0.016	0.006	Bal.
A380.1	8.14	0.64	3.12	0.44	0.22	0.49	0.02	Bal.

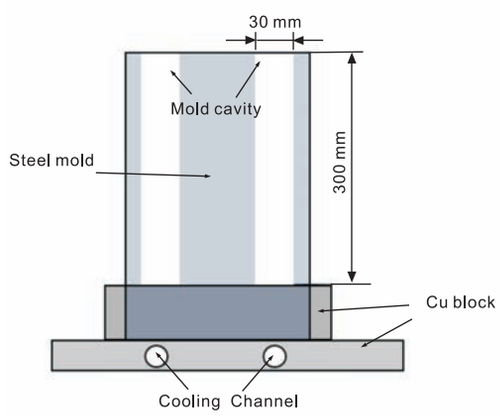

Fig. 1: Directional solidification apparatus used in the experiment

$AlTi_5B_1$ and Al_3B grain refiners were chosen to investigate how the grain refiners affect the porosity formation. The pouring temperature was selected as 740 °C for A356 and A380.1 alloys, and 670 °C for A413 alloy. Two groups of castings were made for each alloy by adding $AlTi_5B_1$ and Al_3B, respectively, as grain refiner. Cast samples were sectioned into five equal parts of 30 mm in diameter and 60 mm in length. Each of these samples was further cut horizontally into two parts of 30 mm in diameter and 10 mm and 50 mm in length, respectively, as shown in Fig. 2. The external shrinkage on the top of each cast specimen was calculated as the volumetric shrinkage.

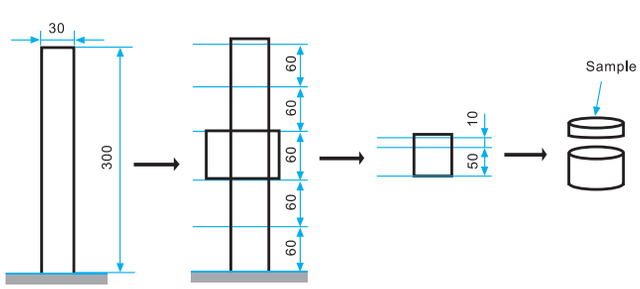

Fig. 2: Preparation of sectioned surfaces of the cast part for examining (mm)

The samples were scanned using a scanner and transformed into an image on a computer. Porosity calculation was done by using the image analysis software SigmaScan. Data obtained from the software were evaluated statistically. Microstructure observation and analysis were performed by using optical microscopy (OM), scanning electron microscopy (SEM) and energy dispersive spectroscopy (EDS) methods.

2 Result and discussion

Macro images of the samples are shown in Fig. 3. These macro images were taken from the same location of different castings. As seen from the images, there is a great difference in the shape, size and distribution of pores, indicating that $AlTi_5B_1$ and Al_3B have completely different effects on the porosity formation and distribution. This effect can be more clearly seen in A356 and A380.1 alloys, but not in A413 because A413 alloy has a eutectic composition. Thus, the planar growth of the eutectic phases pushes the pores (if any) towards solidification direction, and all the porosities in the alloy will be collected in the region of the final solidification area of the casting, i.e., at the top of the cylindrical bars. Also, the lack of freezing range in this alloy is another reason for the lack of pore formation [20].

It is known that the A356 alloy has dendritic and Si-eutectic morphology, whereas, A380.1 alloy has dendritic, Si-eutectic and Cu-eutectic morphologies [21-24]. Different morphologies of these alloys result in the different final properties of cast parts. Representative microstructure images are given in Fig. 4. It can be seen that A356 alloy consists of α-Al dendrites and Al-Si eutectic phase. The Al_3B refined alloy has a more homogeneous dendritic structure than the $AlTi_5B_1$ refined alloy. Dendritic morphology can be seen in the pores of A356 in Fig. 4(g).

According to the research results of Ref. [25], the A413 alloy has only Al-Si eutectic phases. However, α-Al dendrites can be seen in Figs. 4(b) and (e). It appears that the thermal gradient and heat flow result in the nucleation of primary dendrites due to the addition of $AlTi_5B_1$ grain refiners, but in eutectic alloys, dendritic structures are not expected to be seen. They can only form in the case of a change in heat extraction and the presence of grain refiners. Moreover, the Al_3B addition results in the formation of primary silicon.

When it comes to A380.1 alloy, the columnar structure is dominant with $AlTi_5B_1$ addition, and finer equiaxed structure is seen in the alloy with Al_3B addition. In A380.1, pores were found in between the dendrites rather than the eutectic phase

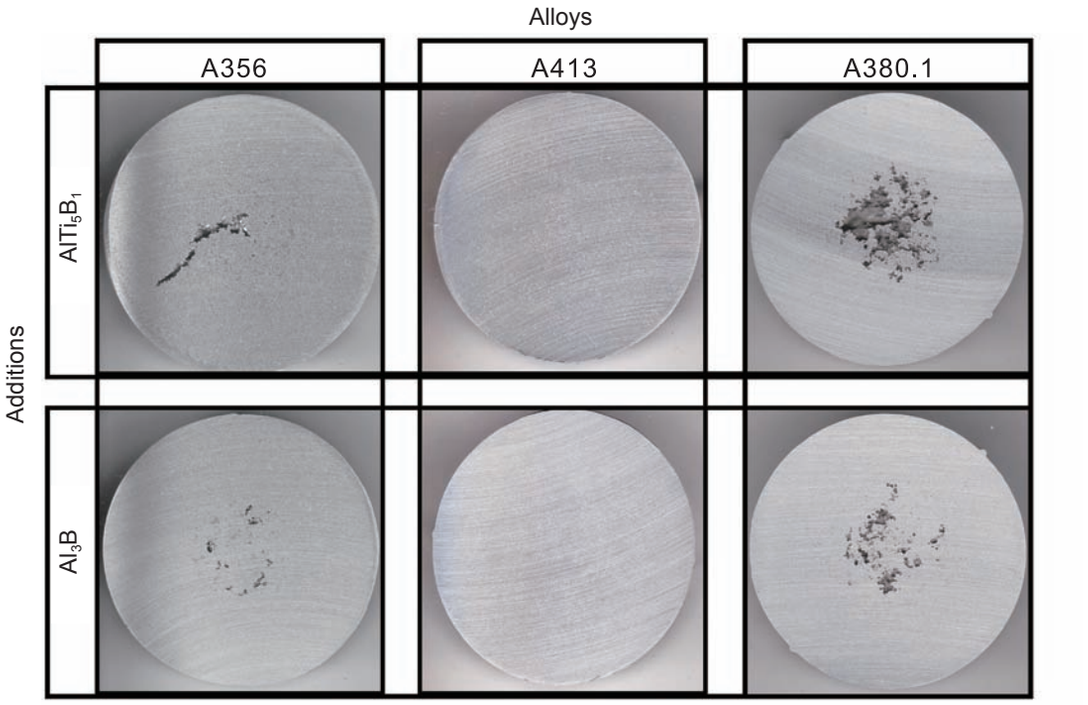

Fig. 3: Macro images of porosity formations in directionally solidified alloys with different grain refiners

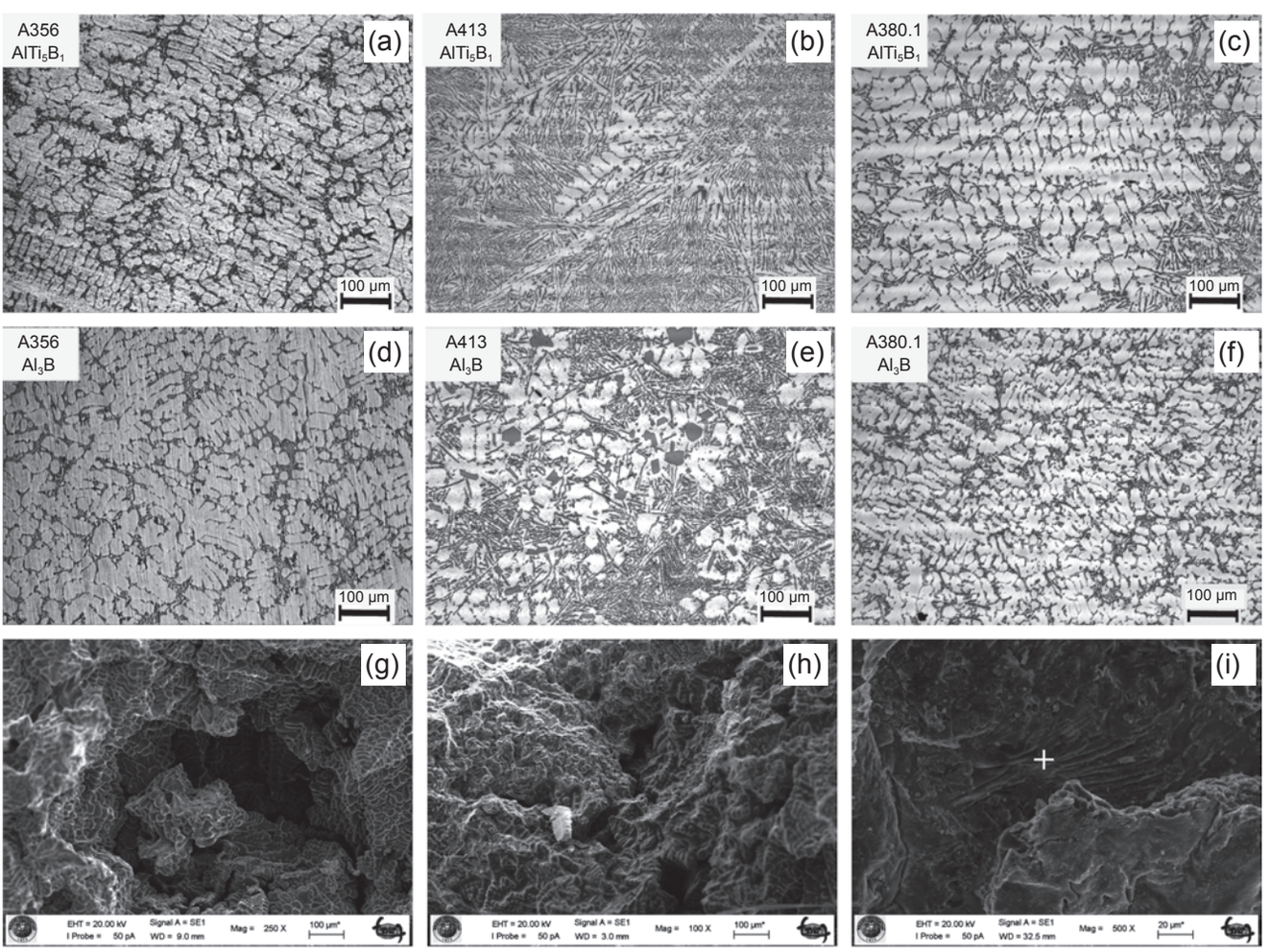

Fig. 4: Representative microstructures (a–f) and SEM images (g–i) of the three alloys refined by $AlTi_5B_1$ (a–c) and Al_3B (d–f)

(Fig. 4h). This indicates that pores are formed prior to eutectic transformation. Zhang et al. [26] claimed that most of the porosities were formed in the eutectic solidification stage. However, in this work, it was found that a thick oxide was present in the pores of A380.1 alloy (Fig. 4i), which is confirmed by the EDS analysis given in Table 2. This supports the fact that pores are formed by the unraveling of bifilms when solidification shrinkage starts; therefore the pores appear between the dendrites, not around or surrounded by the eutectic phase.

Table 2: EDS analysis of a porosity formed by oxide films for the point marked in Fig. 4(i)

Element	wt.%	at.%	Error (%)
Aluminum	66.19	60.24	3.9
Oxygen	9.18	14.10	2.6
Carbon	6.52	13.34	1.9
Copper	6.09	2.35	0.3
Silicon	7.91	6.91	0.5
Magnesium	2.19	2.21	0.2
Iron	1.09	0.48	0.1
Manganese	0.82	0.37	0.1
Total	99.99	100.00	

Image analysis was carried out on the cross-sections of the samples in order to quantify the pores. It can be seen from Figs. 5(a) and (b) that the total length of pores and the total area of pores have almost the same trend for each condition. A413 eutectic alloy has the minimum total area of pores. The difference in the effect of grain refiners can be seen clearly. Al_3B grain refiner has a greater effect on the amount of porosity than the $AlTi_5B_1$ grain refiner. This effect can be seen on A356 and A380.1 alloys more significantly. As shown in Fig. 3, the pores are smaller and accumulated in the center of the samples with Al_3B grain refiner. The grain refiners promote the nucleation of dendrite during solidification and thus decrease the dendrite size. Therefore, the porosity formation might be affected by grain refiners. The solidification rate affects the size and amount of micro porosities [27]. It can also be seen that grain refiners play an important role in the diameter of pores. Figure 5(c) shows that the size of pores of the alloy refined with Al_3B is greater than that with $AlTi_5B_1$. Dispinar [12, 28] concluded that by Al-B grain refinement, more localized and large pores were formed which were attributed to the higher feeding efficiency. The maximum diameter of pores was seen in the A380.1 alloy. A ranking of an average diameter of pores (đ) for alloys can be presented as: $đ_{A380.1} > đ_{A413} > đ_{A356}$.

It can be seen that the average diameter of pores for A413 alloy is almost not affected by grain refiner.

The number density (N), normalized total length (Nđ), total area ($N\pi đ^2/4$) and total volume ($N\pi đ^3/6$) of porosities were calculated to see how the porosity formation changes statistically. The results are given in Figs. 5(e) to 5(g). The results show a similar trend for each condition. The effect of the Al_3B grain refiner on porosity formation seems to be in a decreasing trend from A380.1 to A356 and then A413.

According to the statistical analysis (Fig. 5), there is almost no difference in porosity formation when the alloys are grain refined with Al_3B. However, $AlTi_5B_1$ addition gave different results for A356 and A380.1 alloys. External shrinkage (ES) of the samples that were obtained from directional solidification castings was measured from the top of the samples. Casting

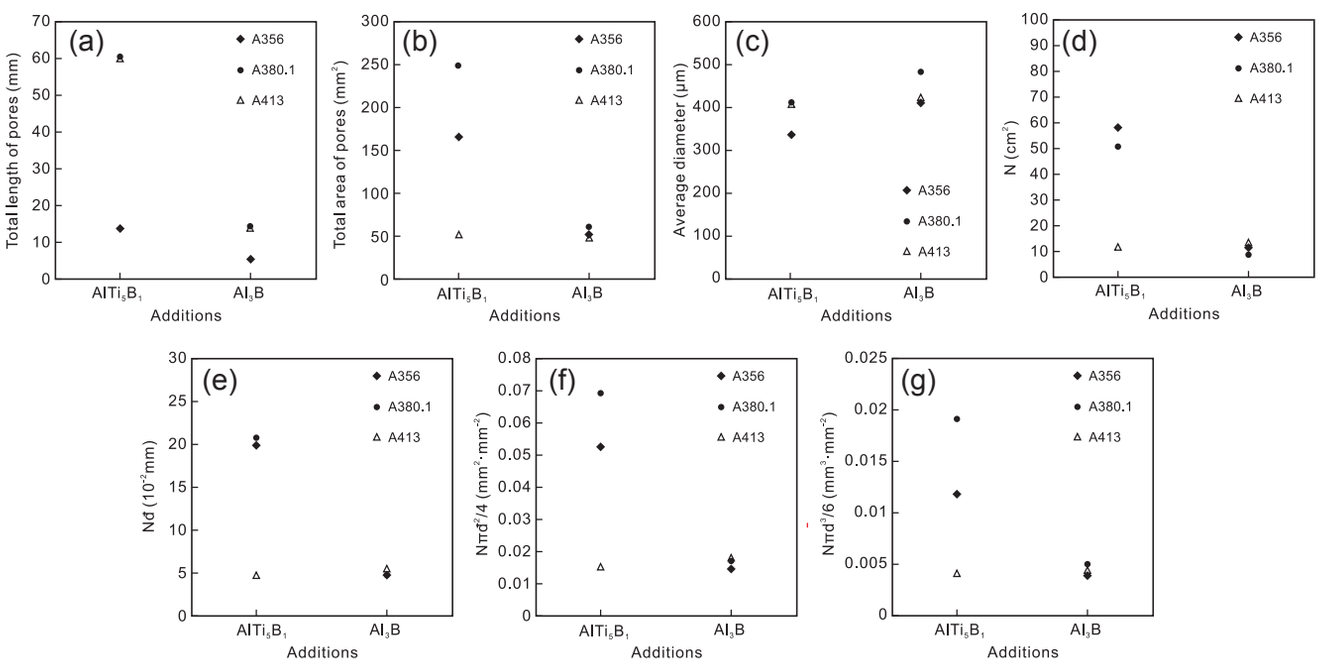

Fig. 5: Relationship between grain refiners and morphological properties of porosities: (a) total length; (b) total area; (c) average diameter; (d) number densities; (e) normalized total length; (f) normalized total area and (g) normalized total volume

images that show ES and schematic representation of measurement and characteristics of ES are given in Fig. 6. It is concluded that there can be a relationship between ES and porosity. As external shrinkage increases, porosity formation decreases. As internal pore formation is decreased, external shrinkage increases. This was discussed in detail by Campbell [1] who claimed that in the absence of bifilms and pore formation in the bulk, the material will exhibit a surface sink.

Sigworth and Kuhn [29] mentioned that each alloy is affected differently by grain refiners. The relationships between ES and different refiners are given in Fig. 7. It can be seen that there is a great difference between results of $AlTi_5B_1$ and Al_3B grain refiners. The ES of Al_3B added castings was more than that of $AlTi_5B_1$. Results of ES can be ranked as follows: $ES_{A356} > ES_{A413} > ES_{A380.1}$, which is in contrast to pores, as shown in Figs. 6 and 7.

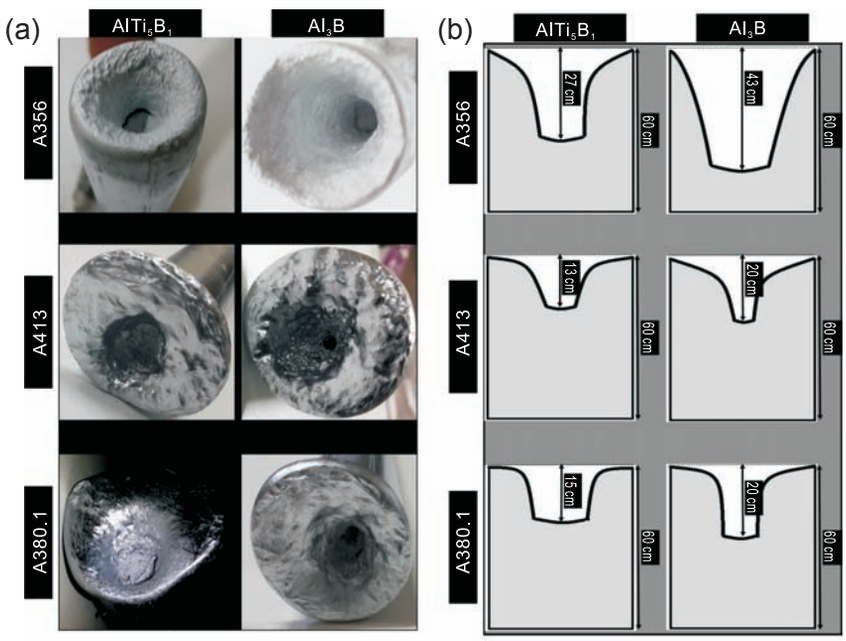

Fig. 6: External shrinkage of directional solidification (a) and schematic images of external shrinkage (b)

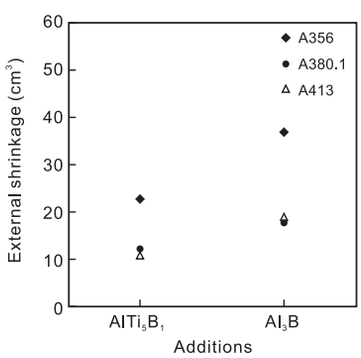

Fig. 7: External shrinkages of castings with different additions

When the average diameters of pores and external shrinkage are considered, it can be seen that there is an inverse ratio between them. As the external shrinkage increases, the diameter of pores decreases.

Distribution of the diameter of pores was investigated by lognormal distribution (Fig. 8). The distribution of the diameter of pores for $AlTi_5B_1$ addition is stable; the distribution of pore diameter for Al_3B addition is scattered. Al_3B grain refiner can result in more larger pores than $AlTi_5B_1$ grain refiner. This result can only be explained by the solidification morphology. The dendritic morphology is finer, columnar and elongated with $AlTi_5B_1$ addition; it is equiaxed and short in

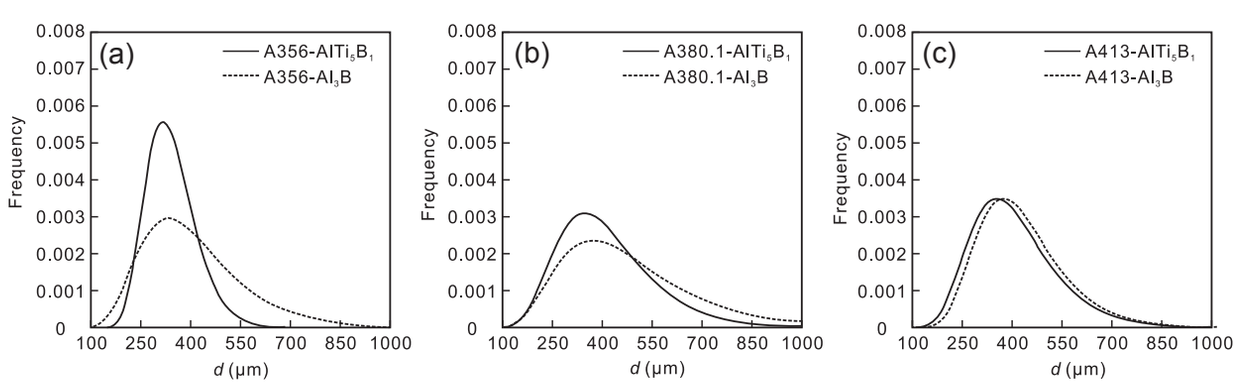

Fig. 8: Lognormal distributions of diameters of porosities: (a) A356, (b) A380.1, (c) A413

Al_3B added castings. Therefore, there would be large number of small pores in the alloy with $AlTi_5B_1$. There is an inverse situation for Al_3B addition.

3 Conclusions

Directional solidification of three alloys (A356, A413 and A380.1) with two different grain refiners ($AlTi_5B_1$ and Al_3B) has been carried out. The porosity formation was investigated widely by calculation of porosity on the cross-sections of cylindrical bars. Statistical analysis was carried out, based on the external shrinkage, and the porosity formation was also evaluated. Conclusions from the experimental work of this study can be made as follows:

(1) Al_3B grain refiner results in a smaller size and number of pores than $AlTi_5B_1$ grain refiner. However, Al_3B has no grain refinement effect on A413 alloy since A413 alloy has a eutectic composition.

(2) There is a relationship between external shrinkage and size and number of porosities. As the size and number of internal porosities decrease, the external shrinkage increases.

(3) There is a significant difference in the distribution of diameter of porosities for $AlTi_5B_1$ and Al_3B added castings.

(4) For A413 alloy, Al_3B addition nucleates the primary silicon, whereas $AlTi_5B_1$ addition nucleates the primary dendrites.

(5) Grain refiners have a different effect on porosity formation of Al-Si alloys with regard to their solidification morphology.

References

[1] Campbell J. Complete casting handbook: metal casting processes, metallurgy, techniques and design. Butterworth-Heinemann, 2015.
[2] Dold P and Benz K W. Rotating magnetic fields: Fluid flow and crystal growth applications. Progress in Crystal Growth and Characterization of Materials, 1999, 38(1): 7–38.
[3] Zimmermann G, Sturz L W and Dagner M J. Effect of melt flow on dendritic growth in AlSi7-based alloys during directional solidification. International Journal of Cast Metals Research, 2009, 22(1–4): 335–338.
[4] Dispinar D and Campbell J. Use of bifilm index as an assessment of liquid metal quality. International Journal of Cast Metals Research, 2006, 19(1): 5–17.
[5] Dispinar D and Campbell J. Determination of aluminium casting quality using bifilm index. In: Proc. Metallurgical and Materials Congress, AFS, 2004.
[6] Emadi D, Gruzleski J E, and Toguri J M. The effect of Na and Sr modification on surface tension and volumetric shrinkage of A356 alloy and their influence on porosity formation. Metallurgical Transactions B, 1993, 24(6): 1055–1063.
[7] Samuel A M, Pennors A, Villeneuve C, et al. Effect of cooling rate and Sr-modification on porosity and Fe-intermetallics formation in Al-6.5%Si-3.5%Cu-Fe alloys. International Journal of Cast Metals Research, 2000, 13(4): 231–253.
[8] Kori S A, Murty B S, and Chakraborty M. Development of an efficient grain refiner for Al-7Si alloy and its modification with strontium. Materials Science and Engineering: A, 2000, 283(1–2): 94–104.
[9] Dong X X, Zhang Y J, Amirkhanlou S, et al. High performance gravity cast Al9Si0.45Mg0.4Cu alloy inoculated with AlB_2 and TiB_2. Journal of Materials Processing Technology, 2018, 252: 604–611.
[10] Sigworth G K and Guzowski M M. Grain refinement of hypoeutectic Al-Si alloy. AFS Transaction, 1985, 93: 907-912.
[11] Wang X M. The formation of AlB_2 in an Al-B master alloy. Journal of Alloys and Compounds, 2005, 403: 283–287.
[12] Dispinar D, Nordmark A, Voje J, et al. Influence of hydrogen content and bi-film index on feeding behaviour of Al-7Si. In: 138th TMS Annual Meeting, Shape Casting: 3rd International Symposium, San Francisco, California, USA, 2009.
[13] Uludağ M and Dispinar D. Assessment of mechanism of pore formation in directionally solidified A356 alloy. Archives of Foundry Engineering, 2017, 17(1): 157–162.
[14] Dong X X, Zhang Y J, and Ji S X. Enhancement of mechanical properties in high silicon gravity cast AlSi9Mg alloy refined by Al3Ti3B master alloy. Materials Science and Engineering: A, 2017, 700: 291–300.
[15] Mostafapoor S, Malekan M, and Emamy M. Thermal analysis study on the grain refinement of Al-15Zn-2.5Mg-2.5Cu alloy. Journal of Thermal Analysis and Calorimetry, 2017, 127(3): 1941–1952.
[16] Yüksel Ç. Weibull analysis of fluidity and hardness of ultrasonically degassed secondary Al7Si0.3Mg aluminum alloy. China Foundry, 2019, 16(5): 352–357.
[17] Yüksel Ç, Öztürk M C, Balcı Y B, et al. Increasing metal quality with ultrasonic degassing method. Technological Applied Sciences, 2017, 13(2): 172–179.
[18] Roy N, Samuel A M, and Samuel F H. Porosity formation in Al-9wt pct Si-3 wt pct Cu alloy systems: Metallographic observations. Metallurgical and Materials Transactions A, 1996, 27(2): 415–429.
[19] Spittle J. Grain refinement in shape casting of aluminium alloys. Taylor & Francis, 2006.
[20] Uludag M, Çetin R and Dispinar D. Freezing range, melt quality, and hot tearing in Al-Si alloys. Metallurgical and Materials Transactions A, 2018, 49(5): 1948–1961.
[21] Boettinger W J, Coriell S R, Greer A L, et al. Solidification microstructures: recent developments, future directions. Acta Materialia, 2000, 48(1): 43-70.
[22] Campbell J. Castings: the new metallurgy of cast metals. Butterworth Heinemann, 2003.
[23] Kurz W, Bezencon C, and Gäumann M. Columnar to equiaxed transition in solidification processing. Science and Technology of Advanced Materials, 2001, 2(1): 185–191.
[24] Sigworth G K. Fundamentals of solidification in aluminum castings. International Journal of Metalcasting, 2014, 8(1): 7–20.
[25] Tsau C H and Yeh J W. The coarsening of silicon particles in a submicron-grained layer-deposited Al-12wt% Si alloy. Materials Chemistry and Physics, 1994, 38(3): 258–266.
[26] Zhang Q Y, Wang T T, Yao Z J, et al. Modeling of hydrogen porosity formation during solidification of dendrites and irregular eutectics in Al-Si alloys. Materialia, 2018. 4: 211–220.
[27] Sigworth G. Understanding quality in aluminum castings. International Journal of Metalcasting, 2011, 5(1): 7–22.
[28] Dispinar D, Ellingsen K, Sabatino M D, et al. Measurement of permeability of A356 aluminium alloys. In: 2nd Int. Conf. Advances in Solidification Processes, Graz, Austrilia, 2008.
[29] Sigworth G K and Kuhn T A. Grain refinement of aluminum casting alloys. International Journal of Metalcasting, 2007, 1(1): 31–40.